Proceedings of the
47th IEEE Conference on Decision and Control
Cancun, Mexico, Dec. 9-11, 2008

Stability Analysis for Liquid Water Accumulation in Low Temperature Fuel Cells

B.A. McCain and A.G. Stefanopoulou and I.V. Kolmanovsky

Abstract— **In this paper we analyze the stability and two-phase dynamics of the equilibrium water distributions inside the porous media of a polymer electrolyte membrane (PEM) fuel cell gas diffusion layer (GDL), which is described with first and second-order parabolic partial differential equations (PDE). A Lyapunov function-based stability criterion is implemented for the liquid mass continuity PDE, while physics and math-based arguments are used to demonstrate a key range of liquid distribution that cannot attain equilibrium.**

The quantity of water within the fuel cell directly affects performance, efficiency, and durability. High membrane humidity is desirable for proton conductivity, yet excess liquid water in the anode has been experimentally shown to be a cause of output voltage degradation. We identify the unstable state(s) representing unbounded growth of liquid water and show that stabilization of channel water mass is sufficient for a stable liquid distribution.

I. Introduction and Motivation

A compact model of the multi-component (oxygen, hydrogen, water), two-phase (vapor and liquid water), spatially-distributed and dynamic behavior across the gas diffusion layer (Fig. 1) is investigated. The time-varying constituent distributions in the GDL of each electrode are described by three second-order parabolic PDEs for reactant (oxygen in the cathode and hydrogen (H_2) in the anode) concentration, water vapor concentration, and liquid water volume. The electrochemical reactions on, and the mass transport through, the catalyst-covered membrane couple the anode and cathode behaviors and, together with the channel conditions, provide the time-varying boundary values for these PDEs. The water (liquid and vapor) PDEs are coupled through the evaporation/condensation rate. Further, the liquid water becomes a nonlinearly distributed parameter that inhibits reactant gas and water vapor diffusion. Liquid water occupies pore space in the GDL, impedes the diffusion of reactant flow towards the membrane, and reduces the fuel cell active area [1], causing performance degradation.

We focus on the stability of the anode GDL water distribution and associated anode channel water mass for two reasons. First, mobile applications of fuel cells spend a considerable time under low-to-medium load conditions, where net water transport is from cathode to anode through the polymer electrolyte membrane. Second, removal of accumulated liquid water is necessary to regain performance, which is typically accomplished by surging an inlet flow

B.A. McCain (bmccain@umich.edu), A.G. Stefanopoulou (annastef@umich.edu), and I.V. Kolmanovsky (ilya@umich.edu) are with the Fuel Cell Control Laboratory, Mech. Engr. Dept., Univ. of Michigan.

Funding is provided from NSF-GOALI CMS-0625610.

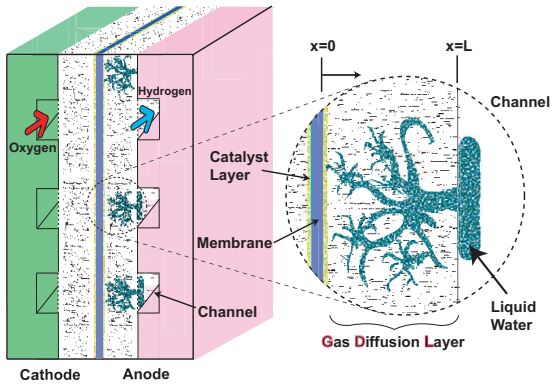

Fig. 1. Conceptual schematic showing accumulation of liquid water in the GDL and subsequent flow to the channel where reactant-blocking film is formed

(e.g. anode H_2 supply), resulting in efficiency loss. Allowing liquid water to accumulate is undesirable for performance, efficiency, and membrane durability reasons, hence estimation and control of the liquid water distribution is critical for effective fuel cell management.

The phenomenon of anode GDL flooding-induced voltage degradation (loss) is addressed in this work, though the methodology presented is applicable to the cathode GDL. In fact, in order to understand and model the anode GDL water accumulation and transport, the cathode water vapor distribution must also be determined because the membrane transport model requires cathode water vapor concentration. Therefore, while the focus is on the anode GDL and channel, the cathode water vapor distribution and channel balance are included supplementally to complete the channel-to-channel model. Finally, since the cathode liquid accumulation does not affect the anode water distributions, it is not modeled and all discussions of liquid refer to that of the anode side.

A. Observation of System Instability

We know from experiment and simulation that the fuel cell will experience unbounded liquid water growth under many normal operating conditions (flow regulated anode inlet, high H_2 utilization, etc). Figure 2 demonstrates the voltage degradation phenomena observed experimentally during dead-ended anode operation (H_2 utilization = 100% between purges); namely that anode flooding is related to voltage degradation.

It turns out that the apparent instability is directly related to the channel water mass state. Specifically, we develop the following result:

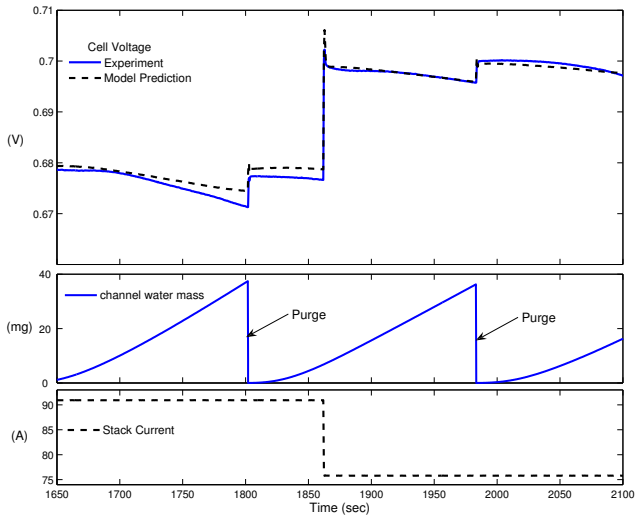

Fig. 2. Experimental results support the hypothesis that anode flooding causes voltage degradation that is recovered through anode channel purging.

Claim: Given the assumptions, partial differential equations and boundary conditions (BC) described in Sec. II, and the analytic solutions from Sec. III, the anode liquid water distribution is stable if the channel liquid water is stabilized.

Sketch of the Proof: The GDL liquid water is locally exponentially stable for fixed channel liquid BC (see Sec. IV). Therefore, stabilization of the channel water mass state results in overall water system stability. Thus if we view the channel water mass as a controlled output, we essentially establish the stability of the resulting infinite-dimensional zero dynamics within the GDL as this output is held constant. We proceed with analysis to justify this result.

II. Fuel Cell Model

Due to space limitations, only a summary of the first principles model will be provided here. The details of the model are identical to those presented in [2]. We proceed with a one-dimensional treatment focusing on the anode, using the following assumptions. The model is spatially isothermal. Gas convective flow in the GDL is neglected. Mass transport is in 1D, normal to the membrane. Water transport out of the anode channel is assumed to be in vapor form.

We designate x as the spatial variable, with x=0 corresponding to the membrane location and x=L corresponding to the anode channel location, and we let t denote time.

The state variables are as follows:

- $c_{H_2}(x,t)$ is the H_2 concentration (mol/m^3) at time t at a cross-section of the GDL located at x, $0 \le x \le L$;
- $c_{v,an}(x,t)$ is the concentration of water vapor at time t at a cross-section of GDL located at x, $0 \le x \le L$;
- The water saturation $s(x,t)$ is the fraction of liquid water volume V_L to the total pore volume V_p, $s = \frac{V_L}{V_p}$. s is thus a concentration-like variable for the liquid water at time t, at a cross-section of GDL located at x, $0 \le x \le L$.

The following intermediate variables are useful:

- $W_l(x,t)$ is the liquid water mass flow (kg/s) at time t at a cross-section of the GDL located at x, $0 \le x \le L$;
- $S(x,t)$ is the reduced water saturation (m^3/m^3) at time t at a cross-section of the GDL located at x, $0 \le x \le L$,

$$S(x,t) = \frac{s(x,t) - s_{im}}{1 - s_{im}}, \tag{1}$$

where it should be noted that $S = 0$ for $s < s_{im}$.

The immobile water saturation s_{im} works as stiction, i.e. there is no liquid flow unless the water saturation s exceeds s_{im}. Finally, the evaporation rate r_v is defined as,

$$r_v(c_{v,an}) = \begin{cases} \gamma\left(c_v^{sat} - c_{v,an}\right) & \text{for } s > 0, \\ \min\left\{0, \gamma(c_v^{sat} - c_{v,an})\right\} & \text{for } s = 0 \end{cases}$$

where γ is the volumetric condensation coefficient and c_v^{sat} is the vapor saturation concentration. Note that evaporation can only occur if there is liquid water ($s > 0$) in the GDL.

Conservation of gas consituents and the liquid mass are employed to determine the three second-order parabolic PDEs that govern the anode reactant, water vapor, and water liquid

$$\frac{\partial c_{H_2}}{\partial t} = \frac{\partial}{\partial x}\left(D_{H_2}^{s_{im}} \frac{\partial c_{H_2}}{\partial x}\right), \tag{2}$$

$$\frac{\partial c_{v,an}}{\partial t} = \frac{\partial}{\partial x}\left(D_v^{s_{im}} \frac{\partial c_{v,an}}{\partial x}\right) + r_v(c_{v,an}), \tag{3}$$

$$\frac{\partial s}{\partial t} = \frac{\partial}{\partial x}\left(b_1 S^{b_2} \frac{\partial S}{\partial x}\right) - \frac{M_v}{\rho_l} r_v(c_{v,an}), \tag{4}$$

where $D_y^{s_{im}}$ is the diffusivity of y inside the GDL porous medium, M_v is the vapor molar mass, and ρ_l is the density of the liquid water.

A. Boundary Conditions

The boundaries for the GDL distributions are at the interfaces with the membrane (x=0) and the channel (x=L). The boundary condition for the reactants at the membrane-GDL interface is a function of the current drawn. Water vapor concentration on one side of the membrane influences the water vapor concentration on the other side, thus there are four BC needed to simultaneously solve both the anode and cathode water vapor concentration second-order PDE. These BC are influenced by inlet flow stoichiometries, temperatures, and relative humidities, as well as the disturbance stack current and the controllable outlet valve on the anode outlet.

For $c_{H_2}(x,t)$, mixed Neumann-Dirichlet type BC are imposed. The channel (ch) boundary condition is,

$$c_{H_2}|_{x=L} = c_{H_2}^{ch} = p_{H_2}^{ch} / \left(\mathcal{R}T\right), \tag{5}$$

where $\mathcal{R}$ is the universal gas constant, T is the temperature, and the H_2 partial pressure in the anode channel, $p_{H_2}^{ch}$, depends on the control input, $\bar{u}$, as discussed in Sec. II-B. The membrane (mb) boundary condition is,

$$\left.\frac{\partial c_{H_2}}{\partial x}\right|_{x=0} = -\frac{1}{D_{H_2}^{s_{im}}|_{x=0}} \cdot \frac{i(t)}{2F} = -\frac{N_{H_2}^{rct}}{D_{H_2}^{s_{im}}|_{x=0}}, \tag{6}$$

where the rct indicates the reaction of H_2 at the anode catalyst, which depends on the current density i (A/m^2), and F is Faraday's constant.

For $c_{v,an}(x,t)$, similar mixed BC are imposed:

$$c_{v,an}|_{x=L} = c^{ch}_{v,an} = p^{ch}_{v,an}/\left(\mathcal{R}T\right), \tag{7}$$

where $p^{ch}_{v,an}$ is the vapor partial pressure in the channel. The slope of the water vapor distribution at the membrane is determined by the water vapor flux across the membrane,

$$\left.\frac{\partial c_{v,an}}{\partial x}\right|_{x=0} = \frac{-N^{mb}}{D^{s_i m}_v}, \tag{8}$$

where the membrane water molar flux N^{mb} is governed by electro-osmotic drag and back diffusion.

For the liquid water PDE, mixed BC are again imposed. Specifically, since water passing into the GDL is in vapor form due to the assumed presence of a micro-porous layer,

$$\left.\frac{\partial S}{\partial x}\right|_{x=0} = 0. \tag{9}$$

The liquid water boundary condition at the GDL-channel interface is an issue of ongoing research. A common assumption is that the hydrophobic nature of the GDL porous media essentially pushes the liquid water into the channel (formed of hydrophillic material) with zero resistance ([3]). On the other hand, Wang and his colleagues ([4],[5]) suggest that the presence of liquid water on the GDL-channel interface constitutes a resistance to flow into the channel. There does not yet exist a physics-based method to relate the amount of liquid water in the channel to resistance to flow from the GDL. In [6], various values of $s(L,t)$ were selected without reason and kept fixed for simulation, and in [5] a constant capillary back-pressure was assumed (7.7kPa) without explanation for the choice.

Here we consider a general form of the liquid boundary condition at the GDL-channel interface:

$$S(L,t) = g(m^{ch}_l(t)), \tag{10}$$

where $m^{ch}_l(t)$ is the mass of liquid water in the channel, and g is an unknown function of that liquid. A form for g is not proposed, and for the purposes of the claims made herein, it is not necessary to know the function. It is assumed, however, that g is monotonically increasing with m^{ch}_l, and has an exponential bound of the form,

$$g(m^{ch}_l(t)) \leq (a - e^{-bm^{ch}_l(t)}), \tag{11}$$

where a and b are positive constants. Thus (10) represents levels of liquid accumulation in the channel such that the GDL liquid boundary condition varies with the quantity present.

B. Anode Channel Equations

For the anode ch, the governing equations for H_2 and water:

$$\begin{aligned} dm^{ch}_{H_2}/dt = &\quad W^{in}_{H_2} - W^{out}_{H_2} + W^{GDL}_{H2}, \\ dm^{ch}_{w}/dt = &\quad W^{GDL}_{w} - (W^{out}_{v} - W^{in}_{v}). \end{aligned} \tag{12}$$

In the general case, the anode will have a humidified inlet stream, with the relative humidity (RH^{in}) and the inlet flow rate ($W^{in}_{H_2}$) prescribed, thus,

$$W^{in}_v = \frac{P^{in}_v}{P^{in}_{H_2}}\frac{M_v}{M_{H_2}}W^{in}_{H_2} \tag{13}$$

where $P^{in}_v = RH^{in}P^{sat}$, and $P^{in}_{H_2}$ is dry inlet gas pressure.

The H_2 and water vapor partial pressures, which represent the channel side GDL BC, are calculated from:

$$\begin{aligned} p^{ch}_{H_2} &= \tfrac{m^{ch}_{H_2}\mathcal{R}T}{M_{H_2}V^{ch}_{an}}, \\ p^{ch}_{v} &= \min\left\{\tfrac{m^{ch}_{v}\mathcal{R}T}{M_v V^{ch}}, p^{sat}_v\right\}, \\ p^{ch} &= p^{ch}_{H_2} + p^{ch}_v. \end{aligned} \tag{14}$$

The anode exit flow rate to the ambient (amb) is modeled as a linearly proportional nozzle equation,

$$W^{out} = \bar{u}\cdot k^{out}(p^{ch} - p^{amb}), \tag{15}$$

where k^{out} is an experimentally determined nozzle orifice constant and $\bar{u}$ is a controllable valve flow $0 \leq \bar{u} \leq 1$ to remove accumulated channel water and, unfortunately, H_2,

$$\begin{aligned} W^{out}_{H_2} &= \frac{m^{ch}_{H_2}}{m^{ch}}W^{out}, \\ W^{out}_{v} &= W^{out} - W^{out}_{H_2}, \end{aligned} \tag{16}$$

where $m^{ch} = m^{ch}_{H_2} + p^{ch}_v V^{ch} M_v/(\mathcal{R}T)$.

The H_2 and water mass flow rate from the GDL to the channel are calculated using:

$$W^{GDL}_{H_2} = -\varepsilon A_{fc} M_{H_2}\left(D^{s_{im}}_{H_2}\frac{\partial c_{H_2}}{\partial x}\right)\Big|_{x=L}, \tag{17}$$

$$W^{GDL}_{w} = -\varepsilon A_{fc}\left(\rho_l b_1 S^{b_2}\frac{\partial S}{\partial x} + M_v D^{s_{im}}_v \frac{\partial c_v}{\partial x}\right)\Big|_{x=L}.$$

III. Analytic Solutions Model

Analysis of the state equations (2)-(4) allowed us in [2] to employ a steady-state analytic solution for the gaseous constituents inside the GDL combined with the numeric implementation of the liquid water state. We call these set of equations as the semi-analytic solution model and will be summarized here, along with analytic solutions for the steady-state liquid water distribution, because it will facilitate the derivation of equilibria distributions and their stability analysis.

A. The Water Vapor Solution

From [2], the steady-state solutions implemented for the cathode and anode GDL water vapor distributions are,

$$c_{v,an}(x,t) = \alpha_1 e^{\beta x} + \alpha_2 e^{-\beta x} + c^{sat}_v, \tag{18}$$

$$c_{v,ca}(x,t) = \nu_1 e^{\beta x} + \nu_2 e^{-\beta x} + c^{sat}_v, \tag{19}$$

$$\text{where}\quad \beta = \sqrt{\gamma/D^{s_{im}}_v}. \tag{20}$$

The α_i and ν_i are functions of the membrane water vapor transport and the channel conditions [2].

B. Liquid Water Governing Equation

An alternate form of the liquid water distribution in the porous medium is obtained by replacing the $c_{v,an}(x,t)$ coupling term in (4) by its steady-state solution (18) (since it has been shown that the time constant of the water vapor is orders of magnitude faster than that of the liquid water),

$$\frac{\partial s}{\partial t} = \frac{\partial}{\partial x}\left(b_1 S^{b_2}\frac{\partial S}{\partial x}\right) + \frac{M_v\gamma}{\rho_l}(\alpha_1 e^{\beta x} + \alpha_2 e^{-\beta x}), \quad (21)$$

for $s \geq s_{im}$, and for $0 < s < s_{im}$:

$$\frac{\partial s}{\partial t} = \frac{M_v\gamma}{\rho_l}(\alpha_1 e^{\beta x} + \alpha_2 e^{-\beta x}). \quad (22)$$

For the $s(x,t) \geq s_{im}$ case, (21) can be integrated twice to obtain the steady-state solution,

$$S_{ss}(x) = \left(\beta_z\left[\beta(\alpha_1-\alpha_2)(x-L) + c_{v,an}^{ch} - c_v^{sat} - (\alpha_1 e^{\beta x} + \alpha_2 e^{-\beta x}) + \frac{S(L,t)^{b_2+1}}{\beta_z}\right]\right)^{\frac{1}{b_2+1}}, \quad (23)$$

where β and α_i are as defined in the $c_{v,an}(x,t)$ solution previously, and $\beta_z = M_v\gamma(b_2+1)/\left(\rho_l\beta^2 b_1\right)$.

For the $0 < s(x,t) < s_{im}$ case, the time-varying solution can be found easily by integrating (22) with respect to time,

$$s(x,t) = \frac{M_v}{\rho_l}\gamma(\alpha_1 e^{\beta x} + \alpha_2 e^{-\beta x})t + s_0(x), \quad (24)$$

where $s_0(x)$ is the water saturation distribution at $t = t_0$. The governing behavior for $0 < s(x,t) < s_{im}$ is such that the water liquid will grow to exceed s_{im} and go back in the 21 case, or will decrease with time and cause all the water liquid to be evaporated ($s = 0$) as discussed in detail in later section.

Figure 3 demonstrates that the steady-state solutions to the water PDEs lead to an exponential form for the vapor and a fractional power polynomial for the liquid. These shapes are highly dependent upon the choice of BC, as evidenced by results from [7], where numeric results show much higher water saturations (s>0.80) at the membrane and zero liquid water at the channel, due to the assumptions of liquid water transport across the membrane and s=0 at the GDL-channel interface. Recent results [8] support the membrane boundary condition (9) used here.

The dash-dot line in Fig. 3 demonstrates that GDL liquid water in excess of the immobile saturation (i.e. flooding) occurs when the water vapor concentration reaches its maximum value of c_v^{sat} in the channel. Under these conditions, the liquid water will grow unbounded in the channel (instability). The solid line represents a lower channel water vapor concentration, and we observe a channel condition ($c_v^{ch} = c_v^{ch*}$) below which the GDL liquid water begins to recede into the GDL. The dotted line depicts the steady-state distributions if $c_v^{ch} < c_v^{ch*}$, where the liquid water front has receded into the GDL (stable with $s(L^-) = 0$).

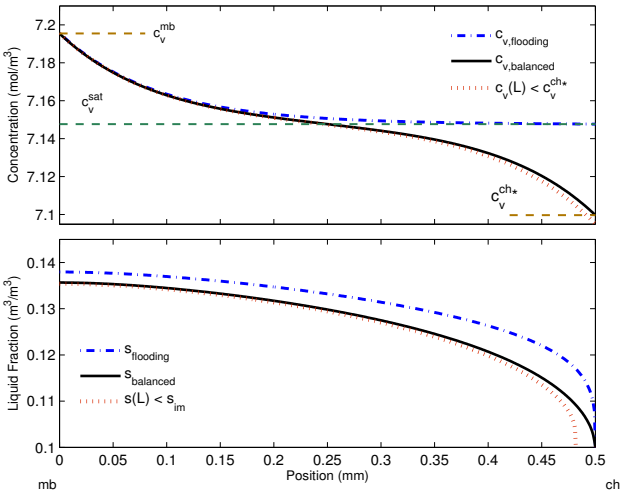

Fig. 3. Anode distribution of liquid water ratio for varying channel water vapor concentrations.

IV. Stability Analysis

We need to show the stability of the liquid water distribution when $s > s_{im}$ for $0 \geq x \geq L$ which will cause a non-zero liquid flow to the channel. We show that if the liquid water in the channel (feeds the boundary condition of the liquid water distribution) is kept stable then the liquid water GDL distribution is also stable. Linearization of the GDL liquid PDE (21) for $s > s_{im}$ is accomplished by substitution of a perturbation from an equilibrium distribution $S(x,t) = S_o(x) + \Delta S$,

$$\frac{\partial s}{\partial t} = \frac{b_1}{(b_2+1)}\frac{\partial^2}{\partial x^2}\left((S_o(x)+\Delta S)^{b_2+1}\right) + f_o(x), \quad (25)$$

where $f_o(x) = \frac{M_v\gamma}{\rho_l}(\alpha_1 e^{\beta x} + \alpha_2 e^{-\beta x})$. A linear approximation for polynomial expansion is,

$$(S_o(x)+\Delta S)^{b_2+1} \simeq S_o(x)^{b_2+1} + (b_2+1)S_o(x)^{b_2}\Delta S. \quad (26)$$

Inserting (26) into (25), it can be seen that the initial steady-state solution is embedded within,

$$\frac{\partial s}{\partial t} = \overbrace{\frac{b_1}{(b_2+1)}\frac{\partial^2}{\partial x^2}S_o(x)^{b_2+1} + f_o(x)}^{\dot{s}_o = 0} + b_1\frac{\partial^2}{\partial x^2}\left(S_o(x)^{b_2}\Delta S\right). \quad (27)$$

Since,

$$\Delta S = \frac{\Delta s}{(1-s_{im})}, \quad (28)$$

we get,

$$\Delta\dot{s} = \frac{b_1}{(1-s_{im})}\frac{\partial^2}{\partial x^2}\left(S_o^{b_2}\Delta s\right) \quad (29)$$

Defining $w \triangleq S_o^{b_2}\Delta s$ results in,

$$w_t = K_2 S_o^{b_2} w_{xx} = \psi(x) w_{xx}, \quad (30)$$

where K_2=$b_1/(1-s_{im})$ and $\psi(x) \triangleq K_2 S_o^{b_2}$.

The BC of the new PDE are found by substituting the original BC into the transformation. At x=0,

$$w_x(0,t) = b_2 S_o^{b_2-1}\frac{\partial S_o}{\partial x}\Delta s + S_o^{b_2}\frac{\partial(\Delta s)}{\partial x} = 0, \quad (31)$$

because both the initial steady-state and perturbation distributions must satisfy the zero-slope requirement at x=0.

For the x=L Dirchlet BC,

$$w(L,t) = S_o^{b_2}(L)\Delta s(L) = 0, \quad (32)$$

because a fixed x=L BC, which is a requirement for steady-state conditions, requires $\Delta s(L)$ remain zero. Thus for any constant boundary condition at x=L, the BC of the transformed system will be zero.

Modifying the steps described in [9] to fit our application, a Lyapunov stability analysis is applied to the plant of the transformed system (30). L=1 is taken for convenience, since a coordinate transformation $z = \frac{x}{L}$ could be implemented without loss of generality.

Using the candidate Lyapunov function,

$$V(w,w_x) = \frac{1}{2}\int_0^1 \frac{w^2(x,t)}{\psi(x)}dx + \frac{1}{2}\int_0^1 w_x^2(x,t)dx, \quad (33)$$

where it should be noted that $\psi(x) \geq 0$ over the range $x \in [0,1]$. Since $\psi(1) = K_2 S_o^{b_2}(1)$ may be zero, for confirmation we check,

$$\frac{w^2(1,t)}{\psi(1)} = \frac{(S_o^{b_2}(1)\Delta s(1))^2}{K_2 S_o^{b_2}(1)} = \frac{S_o^{b_2}(1)\Delta s^2(1)}{K_2} = 0, \quad (34)$$

and thus V is defined over the entire range.

The time derivative of the candidate Lyapunov function,

$$\dot{V} = \int_0^1 \left(\frac{ww_t}{\psi(x)} - \frac{1}{2}\frac{w^2\psi_t(x)}{\psi(x)^2}\right)dx + \int_0^1 w_x w_{tx}dx, \quad (35)$$

where $\psi_t(x) = 0$ since $\psi(x)$ is not a function of time. Substituting the transformed PDE, $w_t = \psi(x)w_{xx}$, and integrating by parts,

$$\dot{V} = \int_0^1 ww_{xx}dx + \int_0^1 w_x w_{tx}dx, \quad (36)$$

$$\dot{V} = ww_x\Big|_0^1 - \int_0^1 w_x^2 dx + w_x w_t\Big|_0^1 - \int_0^1 \psi w_{xx}^2 dx. \quad (37)$$

From (31) and (32) and $w_t(1) = 0$,

$$\dot{V} = -\int_0^1 w_x^2 dx - \int_0^1 \psi w_{xx}^2 dx. \quad (38)$$

Since $\dot{V} \leq 0$, we have stability in the sense of Lyapunov. To show exponential stability, recognize that $0 < \psi_{min} \leq \psi$, and apply Poincare's inequality to show,

$$-\int_0^1 w_x^2 dx \leq -\gamma\psi_{min}\int_0^1 \frac{w^2}{\psi}dx, \quad (39)$$

and

$$-\int_0^1 \psi w_{xx}^2 dx \leq -\gamma\psi_{min}\int_0^1 w_x^2 dx, \quad (40)$$

where $\gamma = \frac{1}{4}$. Then,

$$\dot{V} \leq -\gamma\psi_{min}\left(\int_0^1 \frac{w^2}{\psi}dx + \int_0^1 w_x^2 dx\right), \quad (41)$$

which becomes,

$$\dot{V} \leq -2\gamma\psi_{min}V, \quad (42)$$

indicating that $V \to 0$ exponentially as $t \to \infty$. To show pointwise convergence, use Agmon's inequality (with $w(1,t) = 0$),

$$\max_{x\in[0,1]} |w(x,t)|^2 \leq 2||w(\cdot,t)|| \cdot ||w_x(\cdot,t)||, \quad (43)$$

and the inequality $2||a||\cdot||b|| \leq ||a||^2 + ||b||^2$ to find,

$$\max_{x\in[0,1]} |w(x,t)|^2 \leq ||w(\cdot,t)||^2 + ||w_x(\cdot,t)||^2, \quad (44)$$

where $||\cdot||$ denotes the L2-norm. Since $\psi(x) > 0$ for all x and $V \to 0$, $||w(x,t)|| \to 0$ and $||w_x(x,t)|| \to 0$ as $t \to \infty$, implying,

$$\max_{x\in[0,1]} |w(x,t)| \to 0 \text{ as } t \to \infty. \quad (45)$$

Pointwise convergence is thus shown, and the liquid water distribution within the GDL is exponentially stable.

V. Analysis of Equilibria

The form of (22) suggests that an equilibrium condition for $0 < s(x,t) < s_{im}$ does not exist because the α_i are not functions of s. It is also shown here that the concept of immobile saturation introduces a range of s where equilibrium does not exist.

A. *Claim: No equilibrium solution s exists for which* $0 < s(x) < s_{im}$ *at some x*

We claim that there exists no equilibrium condition such that an $s(x)$ within the GDL is non-zero, but less than the immobile saturation. To see this, we take (4) and substitute the evaporation term,

$$\frac{\partial s(x,t)}{\partial t} = -\frac{M_v\gamma}{\rho_l}(c_v^{sat} - c_v(x)). \quad (46)$$

First, considering the cases where $c_{v,ss}(x) \neq c_v^{sat}$, the RHS of the (46) dynamic equation is not a function of $s(x,t)$, and therefore no condition exists that will satisfy $\partial s/\partial t = 0$. Thus, while $0 < s(x,t) < s_{im}$, $s(x,t)$ will either grow (positive $\partial s/\partial t$, i.e. $c_v(x) > c_v^{sat}$) until it exceeds s_{im}, causing S to be re-introduced as an opposing factor for the condensation or decrease under evaporation (negative $\partial s/\partial t$, i.e. $c_v(x) < c_v^{sat}$), which will cease only when $s(x,t) = 0$.

It remains to show $c_{v,ss}(x) \neq c_v^{sat}$ when $0 < s(x) < s_{im}$.

B. *Claim:* $c_{v,ss}(x) \neq c_v^{sat}$ *for* $0 < s(x) < s_{im}$

We claim that anywhere in the GDL that the liquid saturation steady-state is less than the immobile saturation, the water vapor pressure will not match the saturation pressure. To demonstrate this, we provide a continuity of solution sketch of proof.

This claim can be proven by contradiction. Specifically, if there exists $\bar{x}$ such that $c_{v,ss}(\bar{x}) = c_v^{sat}$ while $0 < s(\bar{x}) < s_{im}$, it can be first shown, by continuity, that $0 < s(x) < s_{im}$

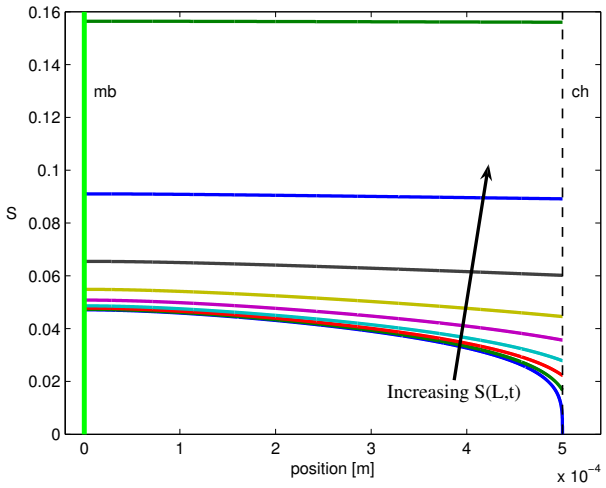

Fig. 4. Example of anode GDL liquid distributions where W_l^{GDL}, as the product of $S^{b_2}(L)$ and $\frac{dS}{dx}|_{x=L}$, reaches equilibrium when $S(L)$ increases by matching W^{mb} with decreased $\frac{dS}{dx}|_{x=L}$.

for all x in an open interval U containing $\bar{x}$. From (18) and (22) it then follows that

$$c_{v,ss}(x) - c_v^{sat} = \alpha_1 e^{\beta x} + \alpha_2 e^{-\beta x} = 0 \;\Rightarrow\; e^{2\beta x} = -\frac{\alpha_1}{\alpha_2} \quad (47)$$

for $x \in U$. Since $\beta \neq 0$, the last relation cannot hold for all $x \in U$ and we reach a contradiction, which implies the truth of Claims **A** and **B**.

VI. Behavior of the Channel Water Mass

In the previous section we showed that the liquid water distribution within the GDL is stable ***if*** the channel water mass has been stabilized. Within the literature, constant values of $S(L,t)$ suggested include $S(L,t)$=0 ([3]); $S(L,t)$=0.01, 0.4, 0.6 ([6]); and $S(L,t)$=0.153 ([5]). Through control of the anode channel outlet valve described in Sec. II-B, using feedback of voltage and relative humidity, it is possible to stabilize the channel liquid mass ([10]). This stabilization can take the form of removal of the channel liquid water (m_l^{ch}=0) or maintenance of channel liquid mass below a predetermined threshold. In either case, the method of Sec. IV can be used to demonstrate stability of the GDL liquid water distribution for typical channel liquid BC found in the literature.

Figure 4 demonstrates the balancing role played by the liquid water transport out of the GDL. As can be seen from (4), the mass flow rate of liquid water is a function of the volume of liquid present ($S(L)$) and the slope of the distribution at the GDL-channel interface ($\frac{dS}{dx}|_{x=L}$). As the $x = L$ BC grows, the magnitude of the slope decreases, with the final value determined by the GDL-channel flow required to balance the liquid mass in the GDL. Thus, for every constant channel BC, the distribution reaches equilibrium, and as $S(L)$ gets larger, the equilibrium distribution flattens to nearly constant.

VII. Conclusions

It has been demonstrated that for a PEM fuel cell model with a GDL liquid water boundary condition coupled to the amount of liquid water in the channel, system liquid water stability can be attained by stabilization of the channel water mass. This is the same result as for the commonly assumed case where the channel liquid has no influence on the GDL liquid. Lyapunov stability analysis is used to show that the liquid water distribution within the anode GDL is locally exponentially stable (does not experience unbounded growth) if the anode channel liquid water mass is bounded. This provides confidence that the stability results are robust to variation in channel BC, as long as those conditions can be stabilized.

Analysis of the GDL liquid water dynamics indicates that the inclusion of an immobile saturation creates a range for which the water saturation s will not reach equilibrium ($0<s<s_{im}$). This result influences stability and control as this unstable region acts as a buffer (delay) to observability of the GDL liquid via the channel water state. While $s(L,t) < s_{im}$, liquid flow from GDL to channel is zero, and therefore the effect of changes to channel water concentration on GDL liquid distribution cannot be observed using measurable outputs (cell voltage, outlet humidity). Feedback control using these outputs must consider this non-equilibrium phenomenon.

References

[1] D. A. McKay, J. B. Siegel, W. T. Ott, and A. G. Stefanopoulou, "Parameterization and prediction of temporal fuel cell voltage behavior during flooding and drying conditions," *J. Power Sources*, vol. 178, no. 1, pp. 207–222, 2008.

[2] B. A. McCain, A. G. Stefanopoulou, and I. V. Kolmanovsky, "A multi-component spatially-distributed model of two-phase flow for estimation and control of fuel cell water dynamics." New Orleans, LA, USA: 46th IEEE CDC, CDC2007-1455, Dec 2007.

[3] J. H. Nam and M. Kaviany, "Effective diffusivity and water-saturation distribution in single- and two-layer PEMFC diffusion medium," *Int. J Heat Mass Transfer*, vol. 46, pp. 4595–4611, 2003.

[4] F. Y. Zhang, X. G. Yang, and C.-Y. Wang, "Liquid water removal from a polymer electrolyte fuel cell," *J. Electrochemical Society*, vol. 153, no. 2, pp. A225–A232, 2006.

[5] P. Sinha and C.-Y. Wang, "Pore-network modeling of liquid water transport in gas diffusion layer of a polymer electrolyte fuel cell," *Electrochimica Acta*, vol. 52, pp. 7936–7945, 2007.

[6] M. Gan and L.-D. Chen, "Analytic solution for two-phase flow in PEMFC gas diffusion layer." Irvine, CA, USA: ASME Fuel Cell 2006, ASMEFC2006-97104, June 2006.

[7] D. Natarajan and T. V. Nguyen, "A two-dimensional, two-phase, multicomponent, transient model for the cathode of a proton exchange membrane fuel cell using conventional gas distributors," *J. Electrochemical Society*, vol. 148, no. 12, pp. A1324–A1335, 2001.

[8] J. P. Owejan, J. E. Owejan, T. W. Tighe, W. Gu, and M. Mathias, "Investigation of fundamental transport mechanism of product water from cathode catalyst layer in PEMFCs." San Diego, CA, USA: 5th Joint ASME/JSME Fluids Engineering Conference, July 2007.

[9] M. Krstic and A. Smyshlyaev, "Boundary control of PDEs: A short course on backstepping designs," *SIAM*, to appear May, 2008.

[10] B. A. McCain, "Modeling and analysis for control of reactant and water distributions in fuel cells," Ph.D. dissertation, Univ. of MI, 2008.